

# Experimental investigation on the thermal performance of a closed oscillating heat pipe in thermal management

Zhonghao Rao<sup>1</sup> · Qingchao Wang<sup>1</sup> · Jiateng Zhao<sup>1</sup> · Congliang Huang<sup>1</sup>

Received: 23 June 2016 / Accepted: 15 March 2017 / Published online: 20 April 2017  
© Springer-Verlag Berlin Heidelberg 2017

**Abstract** To investigate the thermal performance of the closed oscillating heat pipe (OHP) as a passive heat transfer device in thermal management system, the gravitation force, surface tension, cooling section position and inclination angle were discussed with applied heating power ranging from 5 to 65 W. The deionized water was chosen as the working fluid and liquid-filling ratio was  $50 \pm 5\%$ . The operation of the OHP mainly depends on the phase change of the working fluid. The working fluid within the OHP was constantly evaporated and cooled. The results show that the movement of the working fluid was similar to the forced damped mechanical vibration, it has to overcome the capillary resistance force and the stable oscillation should be that the OHP could successful startup. The oscillation frequency slowed and oscillation amplitude decreased when the inclination angle of the OHP increased. However, the thermal resistance increased. With the increment of the heating power, the average temperature of the evaporation and condensation section would be close. If the heating power was further increased, dry-out phenomenon within the OHP would appeared. With the decrement of the L, the start-up heating power also decreased and stable oscillation would be formed.

## List of symbol

D	Diameter of the OHP (mm)
g	Gravity acceleration ( $\text{m s}^{-2}$ )
P	The pressure in the OHP (pa)

T	Temperature (K)
$T_a$	Ambient temperature (K)
R	Thermal resistance ( $\text{K W}^{-1}$ )
L	Length (mm)
A	Total cross-sectional area of OHP
Q	Heat input (W)
h	Convective heat transfer coefficient ( $\text{W m}^{-2} \text{K}^{-1}$ )
$\alpha_n$	Angle ( $^\circ$ )
Ra	Liquid-filled rate
HP	Heating powers (W)
$\nabla T$	Temperature difference (K)
Nu	Nusselt number
Gr	Grashof number
Pr	Prandtl number
B	Constant
U	Voltage (V)
I	Electric current (A)
W	Perimeter (mm)
q	Local heat flux ( $\text{W m}^{-2}$ )
$R_g$	The gas constant
$\Delta P$	Pressure difference (pa)
H	Characteristic length (m)

## Greek symbols

$\rho$	Density ( $\text{kg m}^{-3}$ )
$\sigma$	Surface tension ( $\text{N m}^{-1}$ )
$\nu$	Kinematic viscosity ( $\text{m}^2 \text{s}^{-1}$ )
$e_s$	System uncertainty
$e_r$	Random uncertainty
$\lambda$	Thermal conductivity ( $\text{W m}^{-1} \text{K}^{-1}$ )
a	Thermal diffusivity ( $\text{m}^2 \text{s}^{-1}$ )
x	The fluid displacement (m)
$\phi_0$	The working fluid fill ratio
$h_{fg}$	Latent heat of vaporization ( $\text{J kg}^{-1}$ )
$\mu_l$	Dynamic viscosity ( $\text{N s m}^{-2}$ )

✉ Zhonghao Rao  
raozhonghao@cumt.edu.cn

<sup>1</sup> School of Electrical and Power Engineering, China University of Mining and Technology, Xuzhou 221116, China

$f$	The thermal accommodation coefficient
$V$	The velocity ( $\text{m s}^{-1}$ )

### Subscripts

min	Minimum
max	Maximum
in	Inner
o	Outer
l	Liquid
v	Vapor
e	Evaporation section
c	Condensation section
ip	Input
m, n	Constant
air	Air
eff	Effective
sat	Saturated
cap	Capillary
front	Front contact
back	Back contact

### Acronyms

OHP	Oscillating heat pipe
PCM	Phase change material
CH	Channel

## 1 Introduction

Oscillating heat pipe (OHP), is a well cooling element, which can meet the demands of the increasing heat discharge density in some extreme conditions of electronic devices. It can be divided into three types: (1) open looped, (2) closed looped, (3) closed looped with flow control check valves. As a result of its satisfactory performance, cheap cost and high heat transfer capability, the OHP was introduced as an attractive choice to control the temperature of the electronic devices. The study of the complex internal flow of the OHP is still very challenging. Meanwhile, the heat transfer of the OHP also has not been fully understood.

Raffles and Takayoshi [18] have investigated the bubble generation in the OHP, the phase change phenomena in the evaporation section was studied in detail. The result showed that small driving force produced the liquid slugs and vapor slugs. The slugs movement led to the generation and growth of the bubbles, if the velocity of liquid slugs was lower 0.2 m/s, the tube-size bubble would not be generated. Yan et al. [26] studied the heat transfer behavior of the OHP in rolling motion, they mainly investigated three factors, including the span-wise, transverse and stream-wise additional forces. The first two factors were considered under the low Reynolds number. However, the last

factors were considerably in low Reynolds number. Finally, they concluded that the effect of velocity oscillation period on the OHP performance is more limited than that of Reynolds number and oscillating velocity Reynolds number. Zhao et al. [29] studied the pressure distribution and flow characteristics of an closed OHP with different vacuum degrees. Yin et al. [30] discussed the operation limitation of an OHP.

It is important to control the heat transfer for the electronic components. Yang et al. [27] built a model to investigate the parameter optimization of the OHP for the electronic components. Their model can make well predictions about the startup characteristics of the OHP. Meanwhile, Yong and Luan [28] minutely investigated the startup characteristics of the OHP. Some of the known physics of this system were studied. The results showed that the model in this paper can produce many features of a real system. Cui et al. [4] studied the operation characteristic and heat transfer mechanism of the OHP in detail. They concluded that the thermal resistance was not decreased linearly, but slowdown or even change into rise first before decreasing. Some factors contributed the phenomenon happen in that experiment, maybe the material, structure and inclination of the OHP have influence on the operation characteristic and heat transfer mechanism.

Wang et al. [24] have studied the thermal performance of the OHP using different heating patterns. They mainly studied the unsteady vapor–liquid two-phase flow inside the OHP. The results showed that the OHP can easily startup under a lower filling ratio, meanwhile, the heating patterns have greatly influence on the thermal resistance and the startup process of the OHP. Mameli et al. [12] studied the thermal performance of a closed OHP under different gravity forces. They found that the thermal behavior can be greatly influenced by the gravity when the OHP positioned vertically. And the OHP can undergo a sudden temperature increase in the evaporator section under the microgravity. Such a behavior was not observed in hyper-gravity conditions.

It is generally known that the working fluid has significantly influence on the thermal performance of the OHP. The most common working fluid were water [31], ethanol [3] and acetone [10], or the two mixtures [33]. Riehl and Santos [17] used the water-copper nanofluid in an open loop OHP, adding some solid nanoparticles cloud enhance the thermal performance of the working fluid. They also concluded that the film evaporation effect was more predominant than nucleate boiling under the low heat loads.

In our previous work, the sintered heat pipe was [16] used for the battery thermal management and the experimental result showed that the maximum temperature of the batteries could be controlled below 50 °C, the heat pipes can be well applied to the battery thermal management.

And then, we [15] designed an experiment to apply the OHP to the thermal management of power battery, the results indicated that the OHP can effectively decrease the temperature of the battery packs than the sintered heat pipe, the performance of the battery system was further increased. A phase change material (PCM)/OHP coupled system was built in our previous work [32]. Different influencing factors, including number of turn (3, 4 and 5 turns), thermal conductivity of PCM, flow rate, were considered. This work mainly investigated the heating and cooling process, the whole efficiency of the system.

In order to investigate the thermal performance of oscillating heat pipe in thermal management. The cooling section position, OHP placement and different heating powers were discussed in this paper. The start-up behavior and the temperature oscillations are critically discussed. The results of this experiment will provide a better understanding the performance of the OHP. Meanwhile, the results show that the OHP can be well used in the thermal management.

## 2 Experiment setup and procedure

Aluminum block was used to experimentally simulate a heating pack. It's length and width was 115 mm and 90 mm, respectively. Heating rods, which were connected with a direct-current (DC) power supply (the uncertainty was  $\pm 0.5$  W), were embedded into the aluminum blocks. Different heating powers (5, 15, 25, 35, 45, 55, 65 W) were supplied by the DC power supply. The OHP, was made of copper capillary tube with inner and outer diameters of 2 and 3 mm respectively, was bent into undulating tubes with four turn numbers. Figure 1 shows the charging and vacuum part [25]. The inside vacuum of the OHP was guaranteed by a vacuum pump. The liquid-filled rate of the OHP was maintained at  $50 \pm 5\%$  (volume) in the experiment. The deionized water was chosen as the working fluid of the OHP. The theoretical inner diameter ( $D_{in}$ ) of the OHP in this paper was included in  $D_{max}$  and  $D_{min}$  (the Eq. 2). Figure 1 shows an elementary diagram of the OHP system. Figure 1a shows the OHP system that the OHP was sandwiched between the two aluminum blocks. Figure 1b is an altered version of the lower half of Fig. 1a. The evaporation and condensation section was 90 and 30 mm, respectively. The thermostat bath was used to ensure the inlet water temperature maintained at  $25 \pm 0.05$  °C, the condensation section was immersed in it. However, the evaporation section was clamped between two adjacent aluminum blocks. In order to decrease thermal contact resistance between aluminum blocks and OHP, the thermal silica (ZC-801) was used to bond them. Three OHP orientations including vertical, 45 degree tilt and horizontal were studied. In order to ensure the uncertainty, the K-type thermocouples were

used to measure the temperature of the ice water mixture before the experiment. The temperature of different locations were measure by the K-type thermocouples, which were connected to a Agilent (data acquisition module, 34970 A). CH1,2,3... indicate the temperature channels of the data acquisition module. Figure 1a shows the detail positions of the thermocouples. The temperature of the aluminum blocks were noted by T1–T5. The glass cotton was used to wrap the aluminum blocks to decrease the influence of the environment.

Figure 2 shows the design of different OHP systems in thermal management. The position of the cooling section was clearly seen in this paper,  $L = 9.5, 8.5, 7.5$  and  $6.5$ . The geometric sizes and parameters are summarized in Table 1.

It is generally known that the experiment results may be influenced by system uncertainty (equipment uncertainty and thermocouple uncertainty). Uncertainty  $e$  analysis [9]: the main uncertainties include system uncertainty  $e_s$  and random uncertainty  $e_r$ . The uncertainties of the direct measurement parameters such as  $U$  and  $I$ . The uncertainties of the indirect measurement parameters such as  $T$ ,  $R_{OHP}$ ,  $L$  and  $D_{in}$ . The maximum uncertainties of main parameters are summarized in Table 2.

$$e = \sqrt{e_s^2 + e_r^2} \quad (1)$$

## 3 Conservation equations

The theoretical maximum and minimum inner diameter ( $D_{in}$ ) of the OHP can be calculated by the following equation [8, 9], the actual diameter value must be meet this condition. Otherwise, the heat pipe could not start-up:

$$D_{min} = 0.7 \sqrt{\frac{\sigma}{(\rho_l - \rho_v)g}} \leq D_{in} \leq D_{max} = 2 \sqrt{\frac{\sigma}{(\rho_l - \rho_v)g}} \quad (2)$$

where  $\rho_l$  and  $\rho_v$  are the density of liquid and vapor, respectively.  $D_{in}$  is the inner diameter of OHP. Where  $\sigma$  and  $g$  represent the surface tension and gravity acceleration.

After filling the heat pipe, the slug was formed inside the OHP due to the interaction between gravitation force and surface tension. However, The balance of the gravitation force and surface tension lead to the definition of the Eötvös number (Eo) and Bond number (Bo) [1], the relationship between Eo and Bo is:

$$Eo = \left[ (\rho_l - \rho_v)gL^2 \right] / \sigma = \left( \Delta\rho gL^2 \right) / \sigma = (Bo)^2 \quad (3)$$

For successful pumping action the gravitational force should be lower than surface tension force. Therefore, the Bo should be less than  $2L/D_{max}$ . Here,  $L$  is the total length of the OHP.

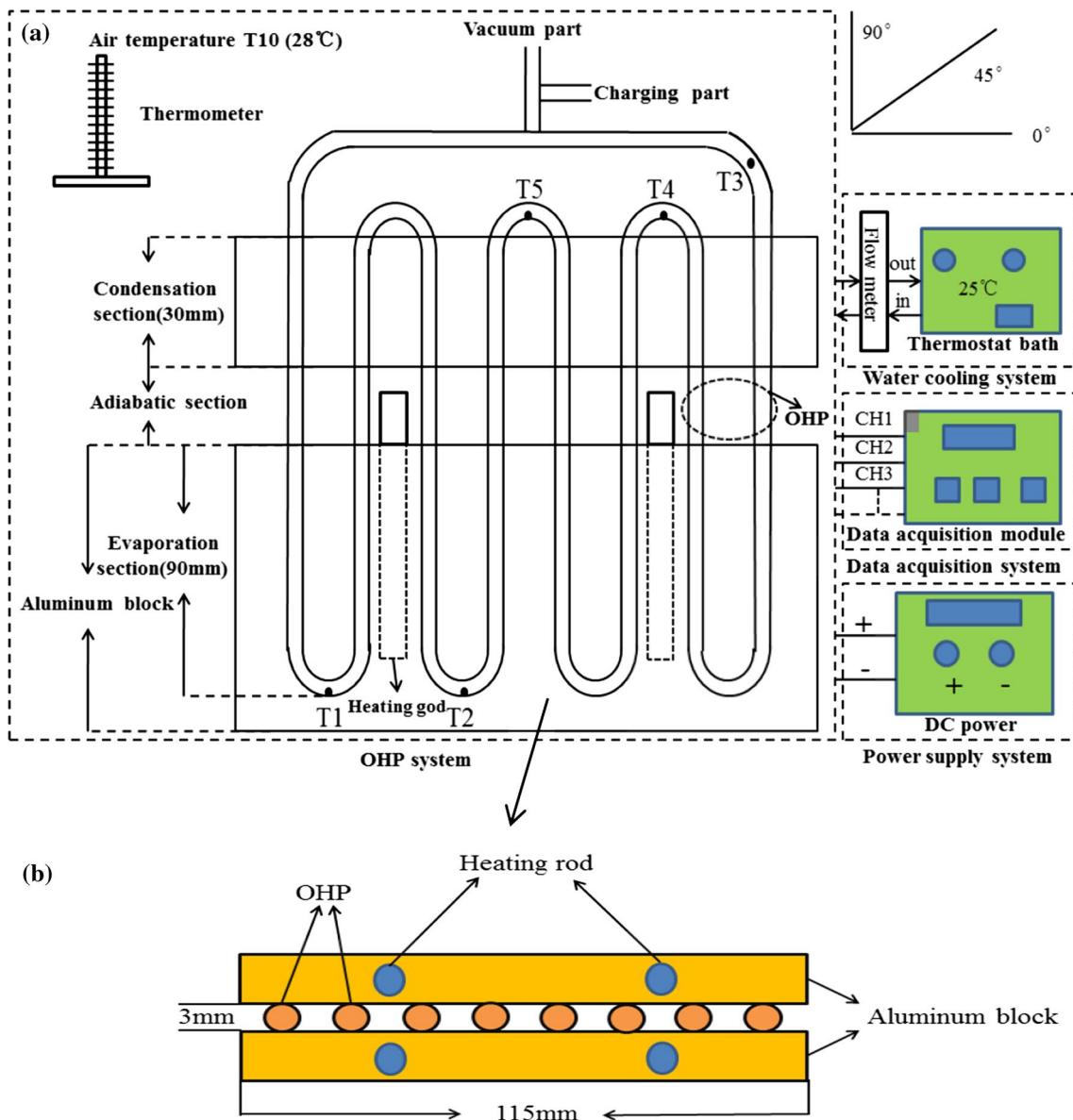


Fig. 1 Details of the OHP experimental set-up

The OHP is a well thermal component. For the evaporation section and condensation section heat exchange, OHP can transfer heat with as little as 1 °C temperature difference. However, the thermal resistance ( $R_{OHP}$ ) has influence on the heat transfer. Simultaneously, there is thermal contact resistance between heating block and OHP. They will disadvantage to the heat transfer. Therefore, some effective methods should be taken to decrease it. Thermal silica is used to decrease the influence of the thermal contact resistance in this study. The OHP thermal resistance can be obtained by the following equation [4]:

$$R_{OHP} = \frac{(T_e - T_c)}{Q_{in}} \tag{4}$$

$$T_e = \frac{T_4 + T_5}{2} \tag{5}$$

$$T_c = \frac{T_1 + T_2 + T_3}{3} \tag{6}$$

$T_e$  and  $T_c$  are the average surface temperatures of the evaporation and the condensation section, respectively.  $T_1$ ,  $T_2$  and  $T_3$  are the temperature of different point in the cooling section.  $T_4$  and  $T_5$  are the temperature of different point in the evaporation. These points can be clearly seen in Fig. 1.

The OHP are applied to many fields due to its high thermal conductivity. The heat pipe can be considered as

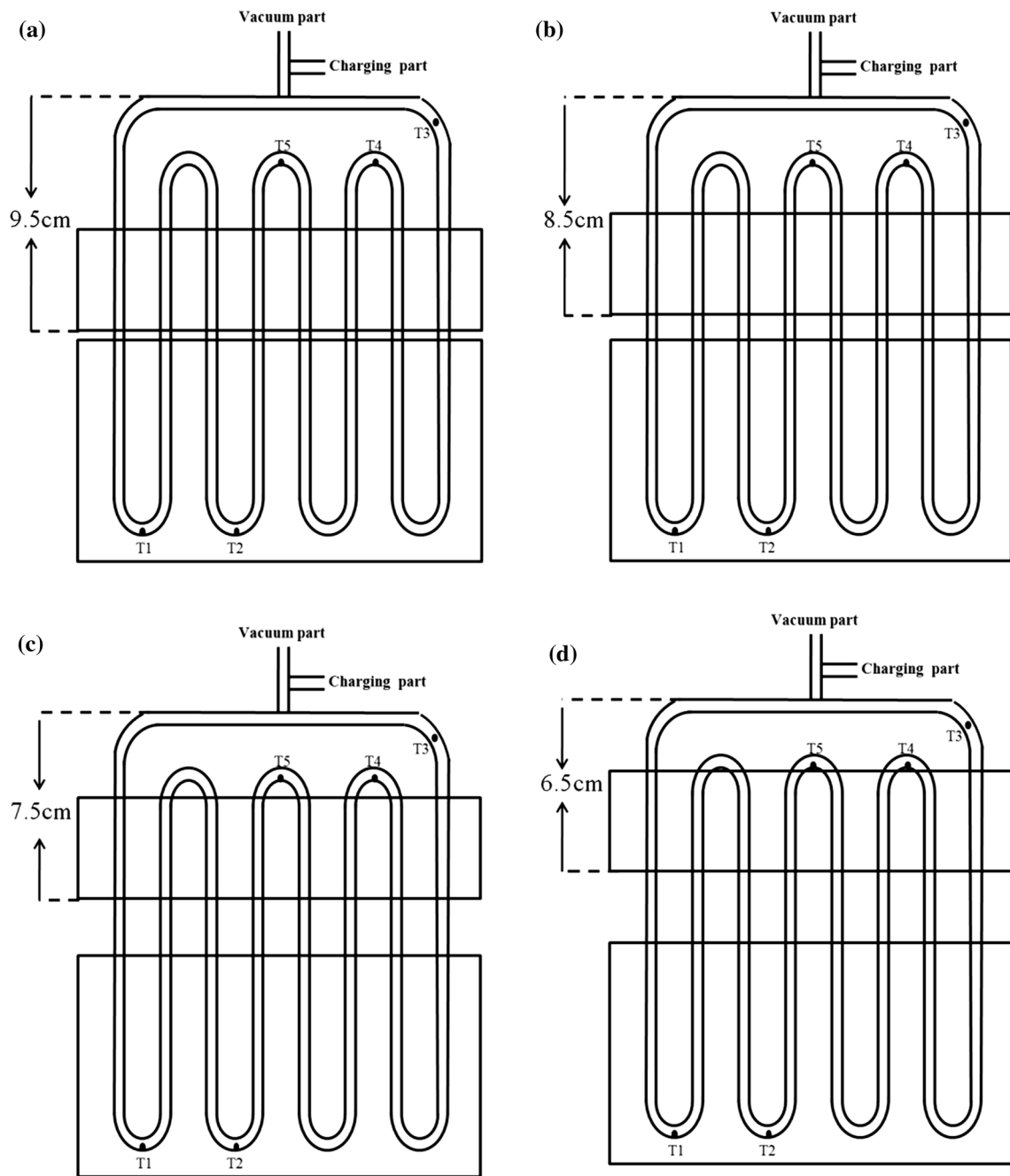


**Fig. 2** Design of different OHP systems

a very high thermal conductive element in energy storage systems [7, 21]. The heat transfer efficiency of the OHP is 400 times higher than that of solid copper. The effective heat conductivity can be calculated as the following equation:

$$k_{eff} = \frac{L_p}{A_1 R_{OHP}} = \frac{Q_{in} L_p}{A_1 (T_e - T_c)} \tag{7}$$

$L_p$  is the length from the center of the heating section to that of the cooling section and  $A_1$  is the total cross-sectional area of OHP. The effective heat conductivity decreases with the increase of the thermal resistance.

The total heat input is  $Q$  in this paper. However, there is heat loss  $Q_1$  in the heating section even though some necessary heat preservation measures are taken. The actual heat input ( $Q_{in}$ ), is smaller than the total heat input, can be calculated. The heat is absorbed by the evaporation, then the

**Table 1** Geometric sizes and parameters

Nomenclature	Parameters	Value
Evaporation section length	$L_e$ (mm)	90
Condensation section length	$L_c$ (mm)	30
Number of turns	N	4
Angle	$A_n$ (°)	0, 45, 90
Cooling water temperature	$T_w$ (K)	$25 \pm 0.05$
Ambient temperature	$T_a$ (K)	$28 \pm 0.05$
Inner diameter	$D_{in}$ (mm)	2
Outer diameter	$D_o$ (mm)	3
Liquid-filled rate	Ra	$50 \pm 5\%$
Aluminum length	$L_a$ (mm)	115
Aluminum width	$W_a$ (mm)	90
Heating powers	HP (W)	15, 25, 35, 45, 55, 65
Cooling section position	L (mm)	65, 75, 85, 95

**Table 2** Maximum uncertainties of main parameters

Parameters	Maximum uncertainties (%)
T	0.2
$T_e$	0.2
$T_c$	0.2
$T_a$	0.2
$T_w$	0.2
L	0.1
$L_e$	0.1
$L_c$	0.1
$L_a$	0.1
$W_a$	0.1
$D_{in}$	0.1
Ra	0.2
P	0.5
$R_{OHP}$	0.6

fluid boils to vapor phase. All of the experiments are carried out under the room temperature. The experiment is considered under the natural convection in an infinite space.

$$Q_1 = hA_1 \nabla T_1 \tag{8}$$

$$h = \frac{Nu \lambda_{air}}{H} \tag{9}$$

$$Nu = B(GrPr)^n_m \tag{10}$$

$$Pr = \nu/a \tag{11}$$

$$Q_{in} = Q - Q_1 \tag{12}$$

where Nu and Gr are Nusselt number (Nu is the ratio of convective to conductive heat transfer across (normal to

the boundary) and Grashof number (Gr is a dimensionless number in fluid dynamics and heat transfer which approximates the ratio of the buoyancy to viscous force acting on a fluid), Pr is Prandtl number (Pr is a dimensionless number, defined as the ratio of momentum diffusivity to thermal diffusivity), B, m, n are constants,  $\nu$  is kinematic viscosity,  $\lambda$  is thermal conductivity,  $a$  is thermal diffusivity,  $h$  is convective heat transfer coefficient,  $H$  is characteristic length.

The heat transfer from inner wall of heat pipe to the outer wall, then vapor condenses to liquid phase, the liquid returns to the evaporation section of the OHP by the gravitation force. The heat ( $Q_2$ ), releasing from the evaporation section, can be calculated as the following equation:

$$Q_2 = 2\pi k_{eff} L_l \frac{T_o - T_{in}}{\ln(D_o - D_{in})} \tag{13}$$

where  $L_l$  is the length of the cooling section. Similarly,  $T_{in}$  and  $T_o$  are the temperature of the inner and outer wall of heat pipe, respectively.  $D_o$  is the outer diameter of OHP.

The heat transferred from the heat pipe to cooling fluid. The heat ( $Q_3$ ) was diffused by the condensation section of heat pipe can be calculated as the following equation:

$$Q_3 = \rho_l \cdot C_l \cdot \mu_l \cdot \Delta T \tag{14}$$

where  $C_l$  and  $\mu_l$  are the specific heat and volume flow rate of water,  $\Delta T$  is the temperature difference of water outlet and inlet,  $\rho_l$  is the density of water.

The heat transfer between the heat pipe and cooling fluid was equal to the heat transfer from inner wall of heat pipe to the outer wall. The input heat also equal to them when the whole device condition is adiabatic.

$$Q_{in} = Q_2 = Q_3 \tag{15}$$

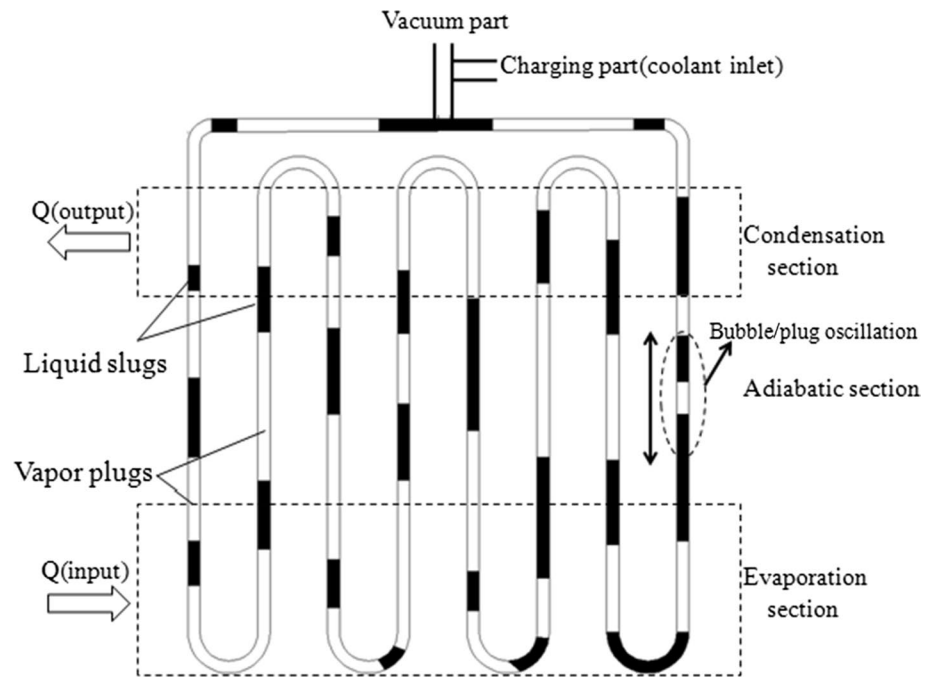
### 4 Results and discussion

Figure 3 shows the schematic of a oscillation heat pipe, the bubble/plug oscillation can be seen inside the OHP. The movement of the liquid and vapor slugs inside the OHP looks like the mechanical vibration. The flowing mathematical model can be utilized to predict the oscillation of the working fluid inside the OHP [10, 34]. The movement equation (Eq. 16) is similar to the forced damped mechanical vibration.

$$\frac{d^2x}{dt} + \left( \frac{8\mu_l W \phi_0}{\rho_l DA} \right) \frac{dx}{dt} + \frac{2A^2 RT_{sat}}{(LA\rho_l \phi_0) \left\{ \left( \frac{L}{2} \right) A\rho_l (1 - \phi_0) / \rho_v \right\}^2} \left[ \left( \frac{L}{2} \right) A\rho_l (1 - \phi_0) + \frac{Q_e}{h_{fg}} t \right] x = 0 \tag{16}$$

Here,  $x$  is the displacement of the movement liquid. Where D, W, L and A are the diameter, perimeter, length

Fig. 3 Schematic of the OHP



and cross sectional area of OHP, respectively,  $\phi_0$  is the working fluid fill ratio.  $Q_e$  and  $h_{fg}$  are the heat transfer quantity and the latent heat of vaporization of working fluid.  $\rho_l$  and  $\rho_v$  are the density of liquid phase and vapor phase under the operating temperature of working fluid;  $T_{sat}$  and  $\mu_l$  are the saturated temperature of working fluid and the dynamic viscosity.

The oscillation and circulation of working fluid in the OHP undergo very complex displacements due to the phase change of the working fluid and interactions between the liquid and vapor plugs. The start-up performance, flow characteristics and thermal performance are three important problems of the application of OHP. The heat transfer within the OHP contain two parts: (1) the latent heat transfer between heating section and cooling section, (2) the sensible heat transfer between the OHP wall and the liquid slugs in the form of a single-phase heat transfer [19]. The interface of the liquid–vapor in the OHP can be divided into three regions: equilibrium thin film region, transition film region and intrinsic meniscus region [5]. It can be contribute to the heat transfer when the  $Q_{in}$  is big enough. The local heat flux of the capillary tube at the interface is obtained as [23]:

$$q = \frac{dQ_{in}}{2\pi(r - \delta)dx} = \frac{T_w - T_{ph}}{\frac{\delta}{k_l} + R_{ph}} \tag{17}$$

$$R_{ph} = \frac{2 - f}{2f} = \frac{T_v \sqrt{2\pi R_g T_v}}{h_v \rho_v} \tag{18}$$

where  $R_{ph}$  is the interfacial heat transfer resistance [20],  $T_{ph}$  is the interface temperature.  $R_g$  is the gas constant.  $f(0.02 \leq f \leq 0.04)$  is the thermal accommodation coefficient, it can be found in [13].  $h_v$  and  $T_v$  is the latent heat of vaporization and the steam temperature, respectively.  $\rho_v$  is the vapor density.  $k_l$  is the thermal conductivity of liquid.  $\delta$  is the thickness of liquid film.  $T_w$  and  $r$  is the temperature of the OHP wall and the inner radius of the OHP, respectively.

The complex flow and heat transfer processes existed at the transition film region.

Heat transfer equation:

$$\begin{cases} V \frac{dV}{dx} + v \frac{dV}{dy} = \frac{V_l}{\rho_l} \frac{d^2V}{dy^2} - \frac{dp_1}{\rho_l dx} + g \\ \frac{dV}{dx} + \frac{dv}{dy} = 0 \\ V \frac{dT}{dx} + v \frac{dT}{dy} = \frac{\lambda}{\rho c_p} \frac{d^2T}{dx^2} \end{cases} \tag{19}$$

Boundary condition [14]:

$$\begin{aligned} y = 0, & \quad V = 0, \quad T = T_w \\ y = \delta, & \quad \frac{dV}{dy} = 0, \quad T = T_{ph} \end{aligned} \tag{20}$$

The velocity distribution can be calculated by Eq. 19 and 20:

$$V(y) = \frac{1}{V_1} \left( \frac{dp_1}{dx} - \rho_1 g \right) \left( \frac{y^2}{2} - \delta y \right) \tag{21}$$

The interfacial equations at the liquid–vapor interface [2]. The mass conservation equation at the liquid–vapor interface can be seen as following equations:

$$\rho_v V_v - \rho_l V_l = (\rho_v - \rho_l) \frac{dN}{dt} \tag{22}$$

Momentum equation:

$$\rho_v \left( V_v - \frac{dN}{dt} \right) V_v - \rho_l \left( V_l - \frac{dN}{dt} \right) V_l = \rho_v - \rho_l + \frac{\sigma}{r} \tag{23}$$

Energy equation:

$$\rho_v \left( V_v - \frac{dN}{dt} \right) h_v - \rho_l \left( V_l - \frac{dN}{dt} \right) h_l = q_v - q_l \tag{24}$$

where  $V$  is the velocity of the normal direction at the interface.  $N$  is position of the liquid–vapor interface.  $t$  and  $h$  are time and enthalpy.  $\sigma$  and  $r$  is the surface tension and the radius of curvature at the liquid–vapor interface, respectively.

Figure 4 shows the movement of the vapor slugs and dynamic contact angle hysteresis [10]. In order to maintain the vapor slugs inside the OHP, the condition inside the OHP should meet the Eq. 25 [11]. Only in such condition the steady movement inside the OHP could be developed. Through the Eqs. 25, 26 and 27, the theoretical inner diameter of OHP can be calculated.

$$\Delta P \geq \Delta P' \tag{25}$$

$$\Delta P' = \rho_l g D_{in} \tag{26}$$

$$\frac{\Delta P \pi D_{in}^2}{4} = \sigma \pi D_{in} \tag{27}$$

The high pressure inside the heating section is caused by the input heat, which is the power source to provide the driving force to drive the fluid flow [22]. Due to the different capillary pressure between plug front and plug end lead to the capillary resistance, the three important influence factors on the different capillary pressure are turn numbers, dynamic contact angle hysteresis and gravity. When the OHP start-up, the gravitation force would be dominant over the surface tension with the OHP placed

vertically. On the contrary, there would have an opposite effect when the OHP placed horizontally. The contact angle depends on the combination of working fluid and the tube wall of OHP. The fluid in the heat pipe has to overcome the capillary resistance force ( $F_{cap}$ ), which can be concluded as the following equation [6]:

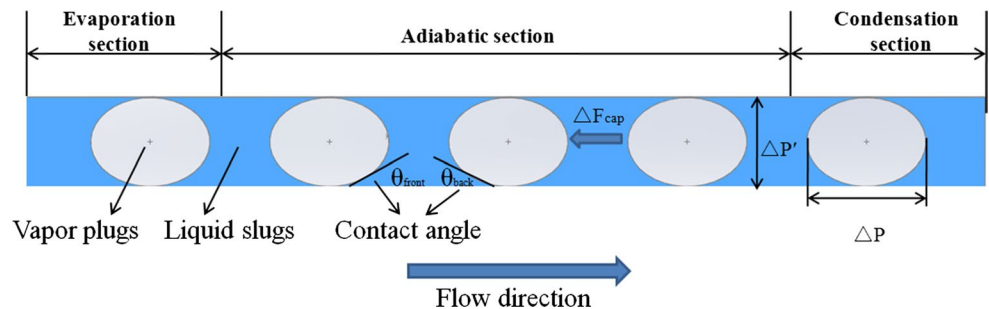
$$F_{cap} = \Delta P_{cap} \cdot \frac{\pi}{4} D_{in}^2 \tag{28}$$

$$\Delta P_{cap} = 4\sigma (\cos\theta_{front} - \cos\theta_{back}) / D_{in} \tag{29}$$

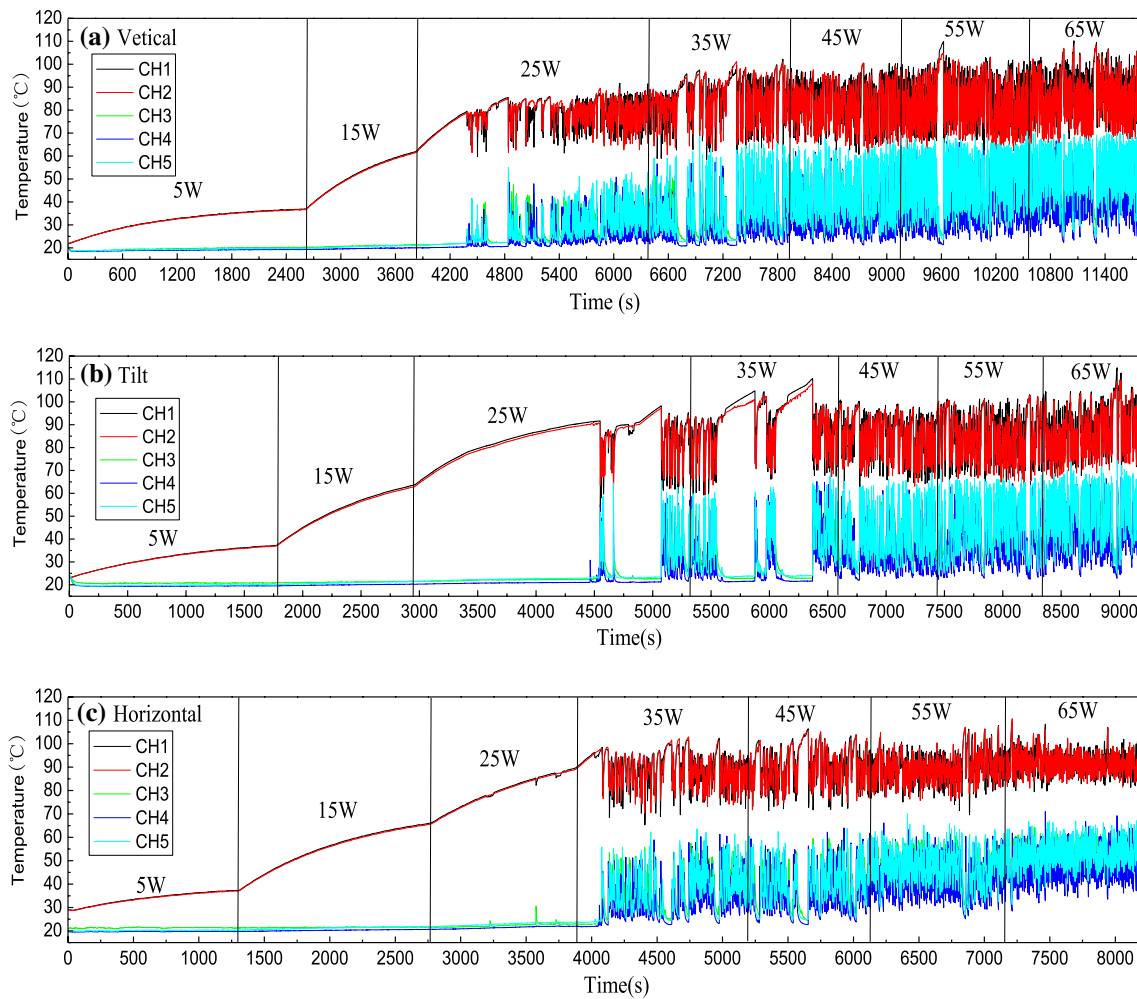
where  $\Delta P_{cap}$  is capillary resistance force per unit area.  $\cos\theta_{front}$  and  $\cos\theta_{back}$  are front contact angle and back contact angle.

Figure 5 shows the temperature variation of the OHP with different directions when the  $L$  was 6.5 cm. The trend of temperature variation likes the forced damped mechanical vibration. When the heating power was 15 W, the OHP did not oscillate, it was just a heat transfer unit. The temperature of the working fluid did not reach the evaporation temperature. As can be seen from Fig. 5a, when the heating power reached 25 W, the OHP begin start-up, the temperature of the start-up was 78.5 °C, the temperature variation with large amplitude and high frequency, the temperature of the evaporation section increased slowly. The surface tension varied with the temperature, therefore, the Bond number also varied. When the OHP start to oscillate, the working fluid would move inside the OHP, which represents the energy transfer, the flow of the working fluid and the heat transfer was complex inside the OHP, the equations of results and discussion section can explain the flow and heat transfer inside the OHP. With the increment of the heating power, the scope of the swing became bigger than before, so did the oscillation frequency. Figure 5b shows the temperature variation with the OHP placed tiltly (45°), the time of the start-up was later than that of the time when the OHP placed vertically, the temperature of the start-up was 91.6 °C. However, we can clearly see the intermittent temperature change,  $\Delta P < \Delta P'$ , the stable oscillation did not formed inside the OHP until the heating power reached 45 W. With the increment of the heating power, the maximum temperature did not increase quickly,

**Fig. 4** Movement of the vapor slugs and dynamic contact angle hysteresis







**Fig. 5** Temperature variation of the OHP with different directions when the L was 6.5 cm

the temperature changed in a range. However, the OHP did not oscillate until the heating power reached 35 W when the OHP was placed horizontally, the temperature of the start-up was 98 °C and the oscillation amplitude was obviously decreased. The heat conductivity of the OHP was low before working fluid evaporated. However, it would be rapidly increased when the OHP start to oscillate. Meanwhile, the temperature difference between  $T_e$  and  $T_c$  decreased, the  $R_{OHP}$  also decreased.

With the increment of the heating power, the maximum temperature did not change much. The reason might be that the heat input at the evaporation section and the heat output at the condensation section achieved a balance. Figure 6 shows the maximum temperature of the OHP with different directions when the L was 9.5 cm. The heat pipe was most easy to oscillate when the OHP placed vertically, the temperature of the oscillation was the lowest among these conditions, and the gravity played a great role in this process. When the working

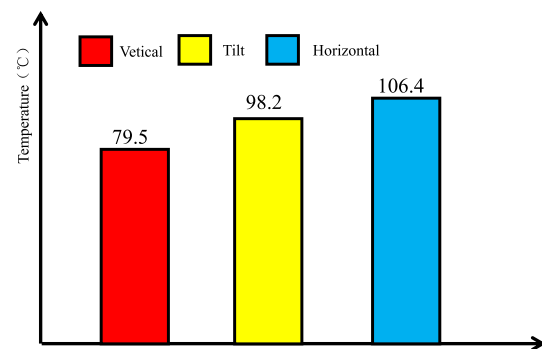


**Fig. 6** The maximum temperature of the OHP with different directions when the L was 9.5 cm

fluid evaporated, the gravitation force would be dominant over the surface tension. However, when the OHP placed horizontally, the backflow of the working fluid would be hindered by the gravitation force, the fluid in

the heat pipe has to overcome the capillary resistance force. Therefore, the oscillation amplitude decreased, the temperature of the oscillation increased. During the oscillating process,  $Q_1$  should be avoided. Therefore, the  $Q_{in}$  would be increased. The  $k_{eff}$  would be also increased. The heat could be transferred to the outside quickly.

Figure 7 shows the temperature variation of the OHP with different directions when the L was 9.5 cm. The oscillating heating power was higher than that of when L was 6.5 cm under the same working condition. The oscillation frequency slowed and oscillation amplitude decreased. As can be seen from Fig. 7, the OHP was easy to oscillate heating power when it was placed vertically. On the contrary, it was hard to oscillate when it was placed horizontally. In previous literature [35], it is also difficult to continue oscillating in the OHP with the angle of  $0^\circ$ . The indirect oscillation in Fig. 7b appeared frequently, the reason might be that

the pressure inside the OHP instability and the flow inside the OHP was very complex. A phenomenon can be seen that the average temperature of the evaporation section did not change significantly. However, the average temperature of the condensation section increased gradually. If the heating powers continue to increase, the average temperature of the evaporation and condensation section would be very close. If the heating power was high enough, the dry-out phenomenon inside the OHP would appear. This condition would be harm to performance of the OHP. Therefore, the OHP should be applied in the corresponding field. The OHP should be placed vertically when it was applied to the thermal management that the gravitation force could overcome the  $F_{cap}$ .

Figure 8 shows the temperature variation of the OHP with different cooling section position when the OHP placed vertically. When the L was 9.5 cm, the oscillation

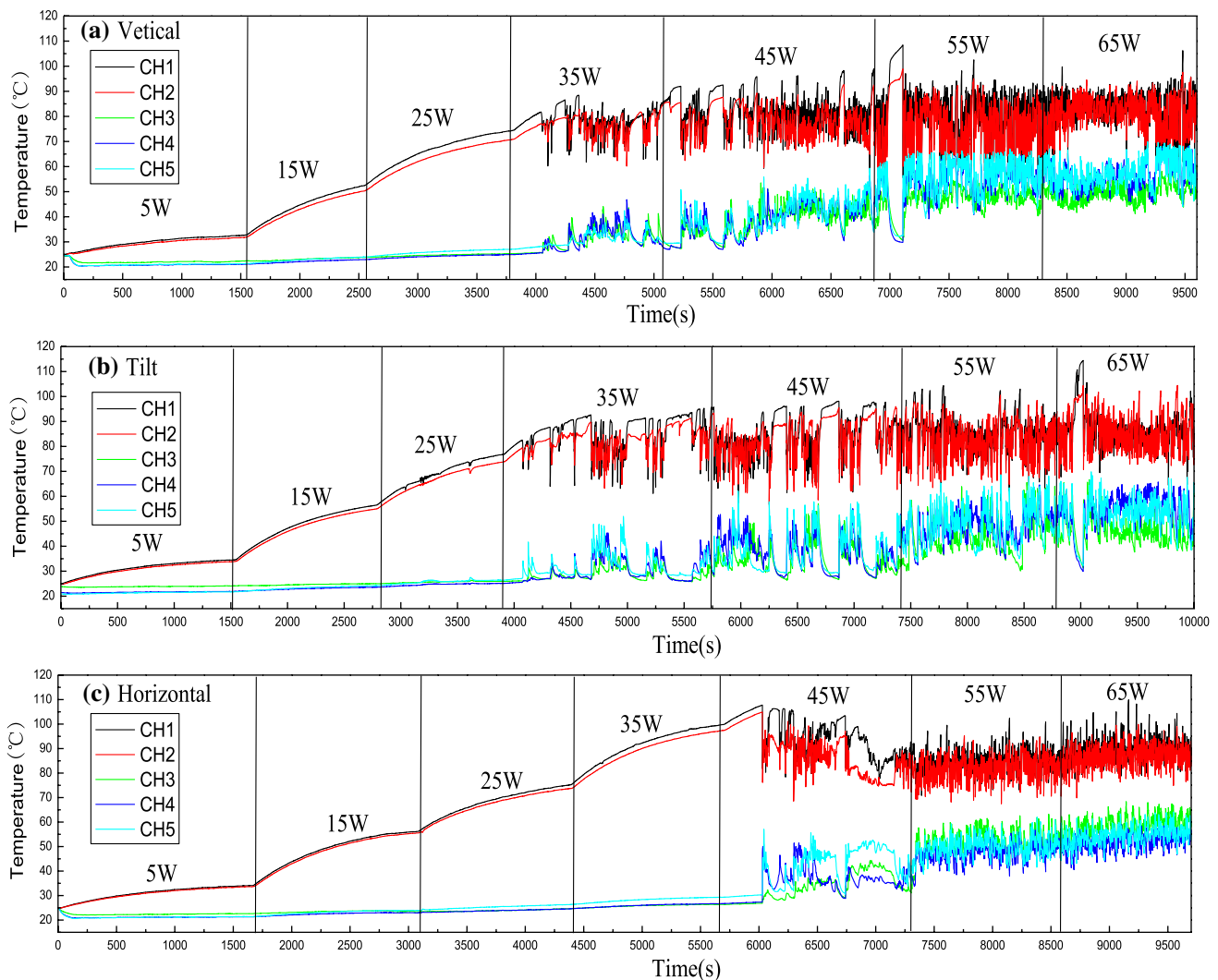


**Fig. 7** Temperature variation of the OHP with different directions when the L was 9.5 cm

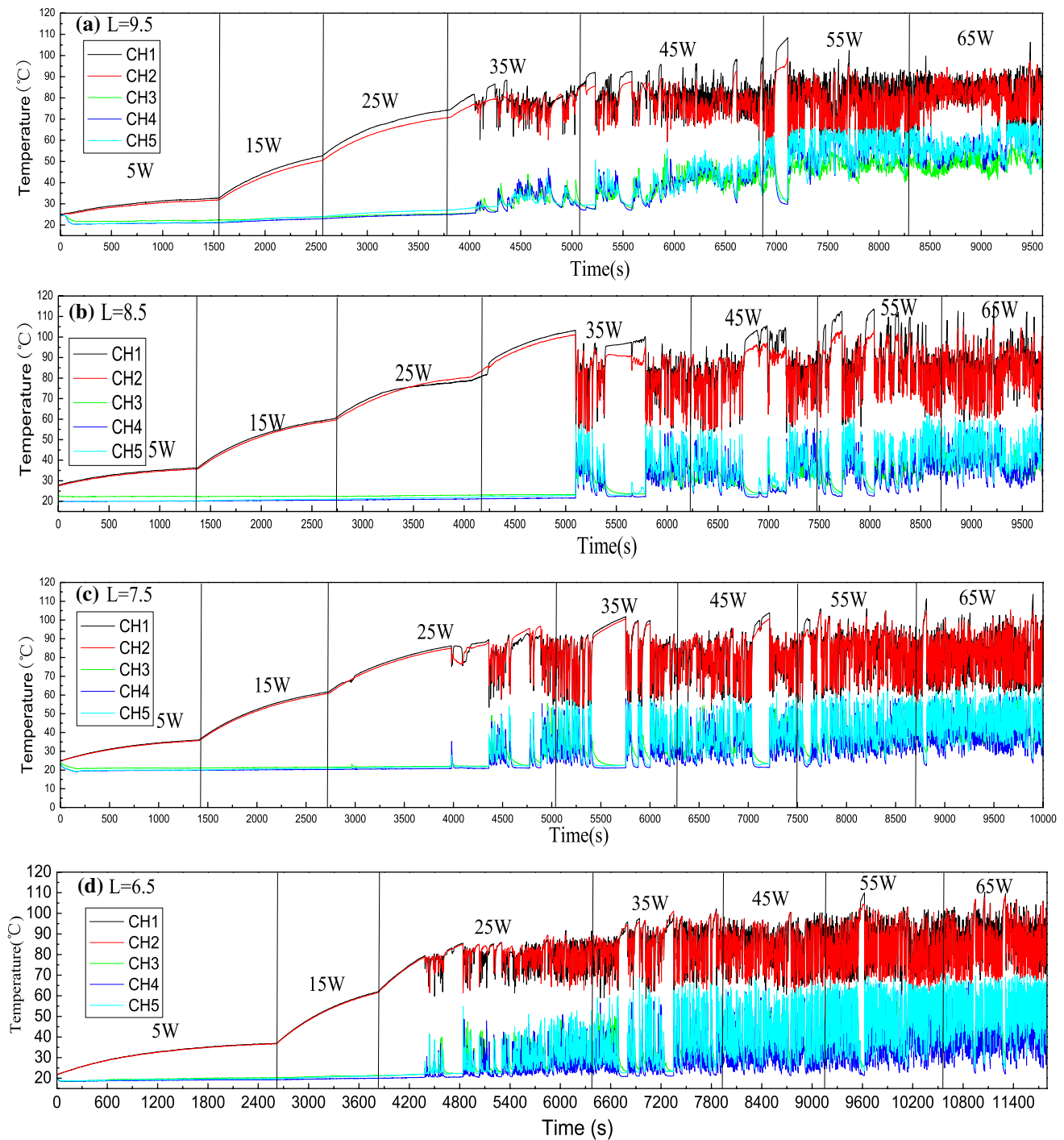


**Fig. 8** Temperature variation of the OHP with different cooling section position when the OHP placed vertically

amplitude was the smallest in these four cases. The condensation section was closed to the evaporation section, once the liquid evaporation, it would be cooled immediately. When the  $L$  was 8.5 cm, the oscillation amplitude increased. However, the oscillation frequency became sparse. When the OHP started, the temperature of the OHP decreased immediately, the temperature oscillation

in a range around. The maximum temperature of the start-up can be seen in Fig. 9. With the decrement of the  $L$ , the oscillation amplitude increased, the temperature of the start-up decreased except when the  $L$  was 9.5 cm. Even though the copper was good thermal conductivity material, the cooling and evaporator section was too close, the absolute adiabatic section did not exist in fact,

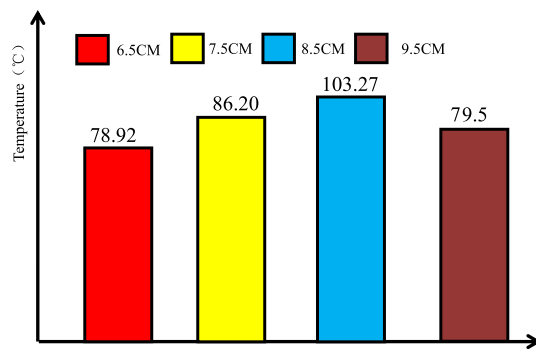


**Fig. 9** The maximum temperature of the OHP with different cooling section position when the OHP placed vertically

ultimately resulting in the temperature of the evaporation section could not increase immediately. The cooling effect will be better when the cooling section away from the evaporation section. The temperature could be controlled by the OHP, which could be applied in the field of the thermal management.

## 5 Conclusions

An experimental investigation was undertaken to study the thermal performance of oscillating heat pipe. This paper presents some new transient experimental data of the closed oscillating heat pipe in terms of condensation and evaporation temperatures. The gravitation force, surface tension, cooling section position and inclination angle were considered in this study. The oscillating behavior and the temperature oscillations are critically discussed. The phase change within the working fluid and the axial oscillation in the OHP prompted the heat transported from the evaporation section to the condensation section. The working fluid inside the OHP was constantly evaporated and cooled. Therefore, the temperature oscillated constantly like the forced damped mechanical vibration. The movement of the working fluid was also similar to the forced damped mechanical vibration. In order to form a stable oscillation, the condition inside the OHP should be  $\Delta P \geq \Delta P'$ . The oscillation frequency slowed and oscillation amplitude decreased with the increment of the inclination angle of the OHP. However, the temperature difference of the OHP increased. Therefore, the thermal resistance increased. With the increment of the heating power, the average temperature of the evaporation and condensation section would be very close. When the heating power is large enough, dry-out phenomenon inside the OHP would be appeared. However, 65 W in this paper cannot able to dry out the working fluid, which is needed further researched. With

the decrement of the L, the stable oscillation would be formed easy inside the OHP and the oscillating heating power was decreased. The condensation section should not be close to the evaporation section. The temperature could be well controlled in a range by the OHP. When the OHP was applied in the thermal management, the OHP should be placed vertically, the working fluid could return by gravity to the evaporation section. The cooling effect could be better than other placement. Although a lot of research has been done to study the OHP, the study of the complex internal flow of the OHP is still very challenging. However, the OHP can be well applied to thermal management. In order to thorough understanding the OHP, the work about the OHP will be further studied in following-on researches.

**Acknowledgements** This work was supported by the National Natural Science Foundation of China (No. 51406223).

## References

- Barua H, Ali M, Nuruzzaman Md, Islam MQ, Feroz CM (2013) Effect of filling ratio on heat transfer characteristics and performance of a closed loop pulsating heat pipe. *Proc Eng* 56:88–95
- Bejan A (2013) *Convection heat transfer*. Wiley, Hoboken, p 729
- Charoensawan P, Khandekar S, Groll M, Terdtoon P (2003) Closed loop pulsating heat pipes: part A: parametric experimental investigations. *Appl Therm Eng* 23(16):2009–2020
- Cui X, Zhu Y, Li Z, Shun S (2014) Combination study of operation characteristics and heat transfer mechanism for pulsating heat pipe. *Appl Therm Eng* 65(1):394–402
- Ha JM, Peterson GP (1996) The interline heat transfer of evaporating thin films along a micro grooved surface. *J Heat Transfer* 118(3):747–755
- Khandekar S, Schneider M, Schafer P, Kulenovic R, Groll M (2003) Thermofluid dynamic study of flat-plate closed-loop pulsating heat pipes. *Microsc Thermophys Eng* 6(4):303–317
- Kim J-S, Bui NH, Kim J-W, Kim J-H, Jung HS (2003) Flow visualization of oscillation characteristics of liquid and vapor flow in the oscillating capillary tube heat pipe. *KSME Int J* 17(10):1507–1519
- Lin Y-H, Kang S-W, Wu T-Y (2009) Fabrication of polydimethylsiloxane (PDMS) pulsating heat pipe. *Appl Therm Eng* 29:573–580
- Liu X, Chen Y, Shi M (2013) Dynamic performance analysis on start-up of closed-loop pulsating heat pipes (CLPHPs). *Int J Therm Sci* 65:224–233
- Ma HB, Hanlon MA, Chen CL (2006) An investigation of oscillating motions in a miniature pulsating heat pipe. *Microfluid Nanofluid* 2(2):171–179
- Maezawa S, Gi KY, Minamisawa A, Akachi H (1995) Thermal performance of capillary tube thermosyphon. In: *Proceeding of the 9th international heat pipe conference Albuquerque, USA*. vol 2, pp 791–795
- Mameli M, Araneo L, Filippeschi S, Marelli L, Testa R, Marengo M (2014) Thermal response of a closed loop pulsating heat pipe under a varying gravity force. *Int J Therm Sci* 80:11–22
- Paul B (1962) Compilation of evaporation coefficients. *ARS J* 32(9):1321–1328

14. Potash M, Wayner PC (1972) Evaporation from a two-dimensional extended meniscus. *Int J Heat Mass Transf* 15(10):1851–1863
15. Rao Z, Huo Y, Liu X (2014) Experimental study of an OHP-cooled thermal management system for electric vehicle power battery. *Exp Therm Fluid Sci* 57:20–26
16. Rao Z, Wang S, Wu M, Lin Z, Li F (2013) Experimental investigation on thermal management of electric vehicle battery with heat pipe. *Energy Convers Manag* 65:92–97
17. Riehl RR, Dos Santos N (2012) Water-copper nanofluid application in an open loop pulsating heat pipe. *Appl Therm Eng* 42:6–10
18. Senjaya R, Inoue T (2013) Bubble generation in oscillating heat pipe. *Appl Therm Eng* 60(1):251–255
19. Shao W, Zhang Y (2011) Effects of film evaporation and condensation on oscillatory flow and heat transfer in an oscillating heat pipe. *J Heat Transf Trans ASME* 133(4):042901–042912
20. Stephan P (1992) Wärmedurchgang bei Verdampfung aus Kapillarrillen in Wärmerohren: Fortschritts-Berichte VDI Reihe 19, Nr. 59. Düsseldorf: VDI Verlag
21. Tiari S, Qiu S, Mahdavi M (2015) Numerical study of finned heat pipe-assisted thermal energy storage system with high temperature phase change material. *Energy Convers Manag* 89:833–842
22. Tong BY, Wong TN, Ooi KT (2001) Closed-loop pulsating heat pipe. *Appl Therm Eng* 21(18):1845–1862
23. Wang J (1999) The analysis on the evaporation heat transfer mechanism within the capillary. *Chem Ind Eng Prog* 50(4):435–442 (in Chinese)
24. Wang J, Wang Z, Li M (2014) Thermal performance of pulsating heat pipes with different heating patterns. *Appl Therm Eng* 64(1):209–212
25. Wang Q, Rao Z, Huo Y, Wang S (2016) Thermal performance of phase change material/oscillating heat pipe-based battery thermal management system. *Int J Therm Sci* 102:9–16
26. Yan BH, Gu HY, Yu L (2012) Heat transfer of pulsating turbulent pipe flow in rolling motion. *Prog Nucl Energy* 59:59–65
27. Yang X-S, Karamanoglu M, Luan T, Koziel S (2014) Mathematical modelling and parameter optimization of pulsating heat pipes. *J Comput Sci* 5(2):119–125
28. Yang X-S, Luan T (2012) Modelling of a pulsating heat pipe and startup asymptotics. *Proc Comput Sci* 9:784–791
29. Yin D, Rajab H, Ma HB (2014) Theoretical analysis of maximum filling ratio in an oscillating heat pipe. *Int J Heat Mass Transf* 74:353–357
30. Yin D, Wang H, Ma HB, Ji YL (2016) Operation limitation of an oscillating heat pipe. *Int J Heat Mass Transf* 94:366–372
31. Zhang XM (2004) Experimental study of a pulsating heat pipe using FC-72, ethanol, and water as working fluids. *Exp Heat Transf* 17(1):47–67
32. Zhao J, Rao Z, Liu C, Li Y (2016) Experimental investigation on thermal performance of phase change material coupled with closed-loop oscillating heat pipe (PCM/CLOHP) used in thermal management. *Appl Therm Eng* 93:90–100
33. Zhu Y, Cui X, Han H, Sun S (2014) The study on the difference of the start-up and heat-transfer performance of the pulsating heat pipe with water—acetone mixtures. *Int J Heat Mass Transf* 77:834–842
34. Zuo ZJ, North MT, Wert KL (2001) High heat flux heat pipe mechanism for cooling of electronics. *IEEE Trans Compon Packag Technol* 24(2):220–225
35. Zhao J, Rao Z, Liu C, Li Y (2016) Experimental study of oscillating heat pipe and phase change materials coupled for thermal energy storage and thermal management. *Int J Heat Mass Transf* 99:252–260